JOURNAL OF CATALYSIS 56, 315–320 (1979)

Metals Chemistry on Hydrotreating Catalysts: NMR and EPR Surveys of Vanadium on Spent Catalyst Materials

B. G. SILBERNAGEL

Corporate Research Laboratories, Exxon Research and Engineering Co., Linden, New Jersey 07036

Received May 19, 1978; accepted October 4, 1978

NMR and EPR techniques are employed to study the chemistry of vanadium deposition on Co–Mo/γ-Al_2O_3 catalysts during the hydrodesulfurization process. A common pattern of deposition is observed, independent of feed and catalyst support type, which consists of the consecutive appearance of three vanadium forms. A vanadyl (VO^{2+}), different from that in the crude oil, dominates at low vanadium levels followed by a diamagnetic, apparently "amorphous" vanadium phase. At high metals loadings (greater than 10 wt%), the dominant form is a sulfide with composition close to V_2S_3.

I. INTRODUCTION

While catalytic desulfurization and demetallization are used for treating many crude oil feeds, rapid catalyst deactivation precludes the application of such techniques to heavier residua. The larger organic molecules and metals (particularly vanadium) which deposit on the catalyst from such residua can eventually affect catalyst activity. We report nuclear magnetic resonance (NMR) and electron paramagnetic resonance (EPR) studies of the types of vanadium species encountered on a series of spent hydrotreating catalysts. Although several preliminary EPR surveys have appeared (*1*, *2*), we believe this to be the first application of NMR to such systems.

We have used observations on a series of model systems synthesized in this laboratory to establish correlations between NMR and EPR resonance parameters and the physical properties of several classes of vanadium compounds and organo-vanadium complexes. These correlations were used, in turn, to examine the discharged catalysts. We find evidence for at least three types of vanadium on the catalysts, the dominant form at high metals loadings being a sulfide of approximate composition V_2S_3.

II. EXPERIMENTAL

NMR and EPR measurements were made on Varian Wideline 112 and Century Series spectrometers, respectively. Vanadium sulfide model samples were prepared by heating appropriate mixtures of the elements (*3*), and wideline NMR has been used to correlate physical properties with composition (*4–8*). EPR studies were performed on samples of Al_2O_3 impregnated with vanadium from NH_4VO_3 and $VOSO_4$ solutions. Both small pore and large pore Co–Mo catalysts were included in the survey. Some were discharged from commercial GO-Fining hydrodesulfurization operations. Others are from test reactors of the Exxon Research and Development Laboratories in Baton Rouge, La. (*9*). These materials were used for hydrodesul-

0021-9517/79/030315-06$02.00/0
Copyright © 1979 by Academic Press, Inc.
All rights of reproduction in any form reserved.

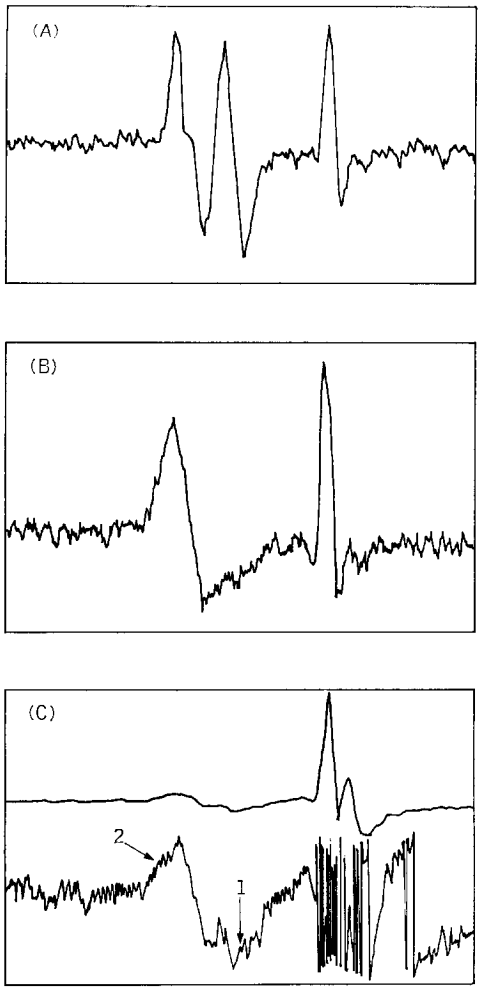

FIG. 1. Comparison of the derivative of the ^{51}V NMR absorption in the model systems V_5S_8 (a) and V_2S_3 (b) with that observed on a spent HDS catalyst (c). A spike, coming from the ^{27}Al NMR of the metal NMR probe is seen in all three spectra. The catalyst trace also contains a ^{27}Al signal from the Al_2O_3 support and two ^{51}V signals: from the diamagnetic vanadium phase (1) and from a vanadium sulfide (2).

furization at typical HDS conditions: temperatures of ~350°C, hydrogen pressures of 2.6 to 16.7 MPa.

Several features of the vanadium NMR spectrum prove very useful in characterizing deposited vanadium species. The *position* of the NMR absorption provides chemical shift information analogous to that obtained in high resolution proton NMR (*7*, *10*), the *shape* of the NMR signal reflects the magnetic and electrostatic environment of the atom. Magnetic properties determine the *temperature dependence* of the shape and shift (*5*), while the *signal intensity* measures the number of atoms in a particular physical or chemical state. For a preliminary study, the shapes of the NMR spectra can be used as "signatures" of different compound types: oxides, sulfides, and carbides have very different signals. Figure 1a and b, the derivative traces of the NMR absorption for V_5S_8 and V_2S_3, shows that very different signatures may occur even for small differences (~8%) in composition. Such variations can often be quantified by detailed measurements within a given chemical class of materials. For example, resonance shifts (often called Knight shifts) are found to vary linearly with composition over a significant portion of the vanadium–sulfur phase diagram, as shown in Fig. 2.

EPR has been extensively used in the studies of vanadyl (VO^{2+}) complexes

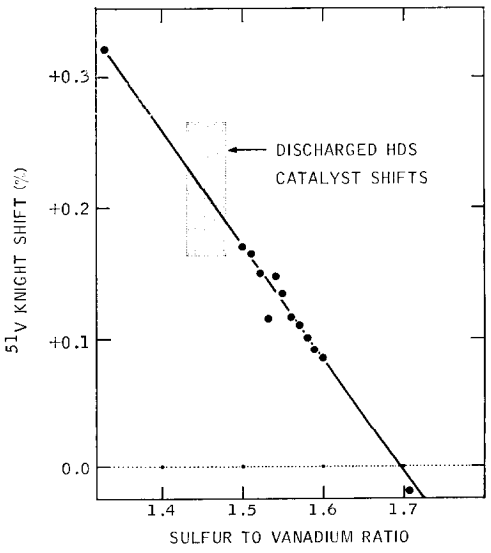

FIG. 2. Correlation of the ^{51}V Knight shift with composition for a series of vanadium sulfides. Shifts observed for sulfides on spent catalysts lie in the shaded region of the figure.

(*11–13*) and crude oils (*14–16*). Use of V_2O_5 as a partial oxidation catalyst has stimulated EPR examination of its magnetic surface defects (*17*, *18*). A recent study indicates that there is a strong correlation between the anisotropy of the EPR parameters and the coordination chemistry of the vanadyl complex (*19*). One form of this correlation is shown in Fig. 3.

III. RESULTS

NMR observations on samples with vanadium loadings of ~5 wt% show an absorption of irregular shape with nearly zero Knight shift. The observability of the signal and the small chemical shift both indicate that the vanadium species contributing to this signal is diamagnetic. An irregular line shape of the type observed would be expected if the vanadium species occupied a series of inequivalent sites. If the geometry and type of neighbors to a vanadium atom vary, the electric quadrupole moment of the vanadium nucleus

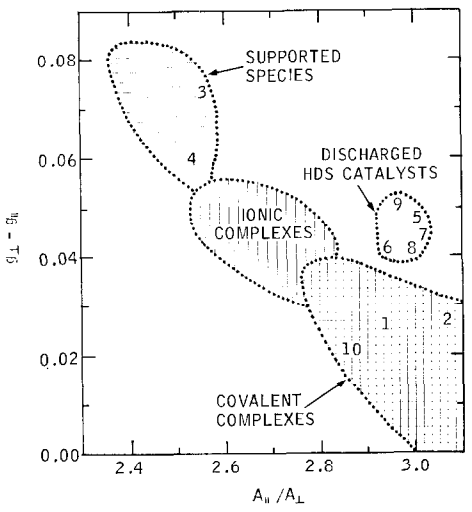

FIG. 3. Correlation of anisotropies in g factor and hyperfine coupling constant for the VO^{2+} EPR in a series of vanadyl complexes (*19*), ranging from covalent species (like VO^{2+} porphyrins) to ionic species (like $VO(H_2O)_5^{2+}$ to VO^{2+} species on supports. Appropriate values for the data of Table 1 are listed in the figure. Note the unique position of the VO^{2+} EPR signal in spent HDS catalysts.

would interact differently with the different environments, producing this type of "smearing" effect. The same irregular shape of the resonance absorption is observed on discharged catalysts run with all feed types. It is the predominant feature of the ^{51}V NMR spectrum at low loadings and remains approximately constant in magnitude for vanadium levels in excess of ~10 wt%.

A second ^{51}V NMR signal appears at higher loadings. While there is little evidence for its occurrence at lower loadings, it becomes the dominant feature in heavily metallized catalysts. A derivative NMR trace showing a catalyst with ~15 to 20 wt% vanadium is shown in Fig. 1c. The two traces displayed show the same data at different levels of gain. To the right of the spectrum is the spike from the ^{27}Al metal of the probe (seen before in Fig. 1a and b) and at slightly higher field the ^{27}Al absorption from the γ-Al_2O_3 support. The vanadium absorptions are seen at lower field. The component labeled *1* represents the diamagnetic phase encountered at low concentration, while component *2* is the high concentration signal. By comparison with Fig. 1b, the shape of component *2* is seen to be very similar to V_2S_3. A more definitive assessment of the composition is obtained from a comparison of the shifts of the spectrum with those deduced from model system studies. The shift of component *2* is independent of metals loading for samples from the same reactor and varies from ~0.19 to ~0.23% for samples from different runs. Using the shift-composition correlation, S/V ratios between 1.43 and 1.48 are implied, as shown in Fig. 2. The range of compositions inferred from these observations is very narrow, ~3%, and lies close to V_2S_3.

The correlation between the amount of vanadium in this V–S phase and the total amount of vanadium on the catalyst can be obtained by comparing the ratio of the ^{51}V and ^{27}Al NMR signals from "V_2S_3" and

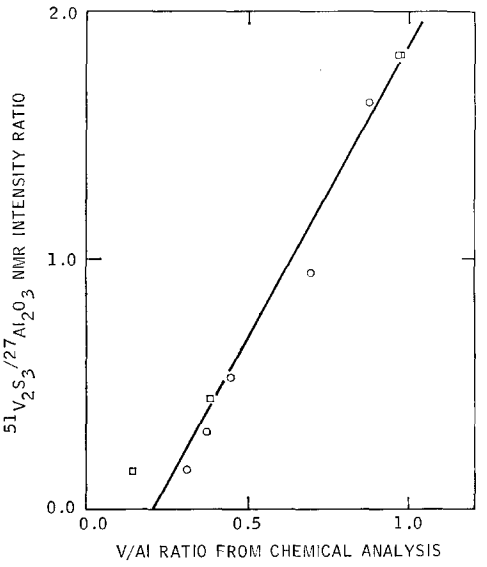

FIG. 4. Variation of ^{51}V NMR intensity vs loading for the vanadium sulfide phase. The aluminum in the γ-Al_2O_3 support is employed as a reference for both the NMR and chemical analysis.

Al_2O_3 with the V/Al ratio obtained from chemical analysis for a series of samples of different metals loadings. At high V/Al loadings, linear relationship is observed (Fig. 4), while the ratio of the ^{51}V NMR of component *1* to that of $^{27}Al_2O_3$ remains approximately constant. The linear "V_2S_3" correlation extrapolates to zero at ~10 wt% vanadium loading suggesting that the diamagnetic component is the dominant form at lower loadings.

The EPR observations demonstrate a change in the paramagnetic species upon deposition. In the crude oil (Fig. 5a) a narrow, well-articulated, 16-component hyperfine spectrum is observed, typical of VO^{2+} in a porphyrinic complex (*15*). On the catalyst (Fig. 5b), this hyperfine structure still appears, but the components of the spectrum are significantly broadened. The broadening observed does not depend on the degree of vanadium loading or the presence of cobalt and molybdenum on the catalysts. At low loading (~0.3 wt%) at least half of the vanadyl species in the crude oil occurs in this vanadyl form on the catalyst. The EPR parameters, g factors, and hyperfine coupling constants are obtained from analysis of inflection points and zero crossings in the spectra.

In addition to the broadening of the hyperfine structure of the VO^{2+} EPR, seen in Fig. 5a and b, a quantitative change in both the g factors and hyperfine coupling constants occurs upon deposition. A series of present and previous observations is presented in Table 1. A feed like Tia Juana Medium residuum has EPR parameters comparable to those of VO^{2+} porphyrin and other crude oils (entries 1 and 2 of Table 1). By contrast (entries 6–9), different g factors and hyperfine coupling constants are seen for the deposited vanadyl, which is independent of the feed type used for processing. Comparison with vanadium artificially deposited on SiO_2 and Al_2O_3 catalysts and calcined (entries 3 and 4), shows that the species deposited under HDS conditions is different from that as well. However, the VO^{2+} signal seen on the spent catalyst is nearly identical to that observed when a calcined catalyst is subsequently sulfided, suggesting that both the support and sulfur are part of the VO^{2+}

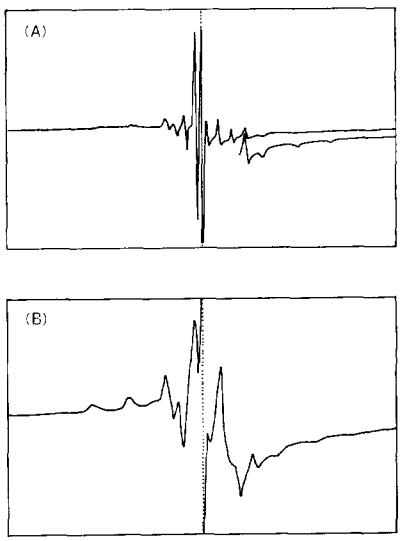

FIG. 5. VO^{2+} EPR absorption derivatives for crude oil (a) and the spent catalyst (b).

TABLE 1

VO^{2+} EPR Resonance Parameters

	$g_{\parallel}$	$g_{\perp}$	$A_{\parallel}$ (gauss)	$A_{\perp}$ (gauss)	Reference
1. VO^{2+} porphyrin in THF	1.964	1.989	170.55	58.10	*11*
2. Tia Juana Medium residuum	1.953 ± 0.001	1.980 ± 0.001	171.5 ± 0.7	55.3 ± 0.4	[a]
3. VO^{2+} on γ-Al_2O_3 (calcined)	1.916	1.989	181.2	70.75	*18*
4. VO^{2+} on SiO_2 (calcined)	1.922	1.982	195.1	77.2	*18*
5. $VOSO_4$ on Al_2O_3 (sulfided)[b]	1.920 ± 0.005	1.966 ± 0.001	193.4 ± 3.2	64.3 ± 0.8	[a]
6. GO-Fining catalyst A	1.926 ± 0.001	1.966 ± 0.001	196.9 ± 0.6	66.8 ± 0.2	[a]
7. GO-Fining catalyst B	1.926 ± 0.002	1.972 ± 0.002	193.9 ± 0.9	64.2 ± 1.0	[a]
8. Residfining catalyst A	1.924 ± 0.002	1.964 ± 0.001	194.9 ± 1.0	64.8 ± 0.6	[a]
9. Residfining catalyst B	1.920 ± 0.003	1.972 ± 0.002	197.2 ± 1.3	66.5 ± 0.8	[a]
10. HDS catalyst [Nikishenko *et al.*)	1.964	1.985	160	56	*2*

[a] Present work, errors represent the standard deviation of values determined by independent analyses of the EPR satellites.

[b] Prepared by Dr. T. A. Pecoraro, Exxon Research and Engineering Co.

site. These present observations are at variance with a previous report (*2*) in which the deposited vanadium was claimed to be identical to that in the crude oil. For runs on highly asphaltenic feeds a second EPR spectrum with parameters close to the crude oil values is sometimes observed, which is associated with asphaltenes entrained in the catalyst. This has also been reported by Kwan *et al.* (*1*). These EPR observations can be summarized graphically by referral to Fig. 3, where the individual entries in Table 1 are included in the correlation plot. The discharged catalysts have a VO^{2+} EPR spectrum which is distinct from calcined supported species or covalent complexes of the porphyrin type. The close proximity of the model system data (entry 5) suggests that sulfur is a component of the VO^{2+} complex encountered on the catalyst surface.

IV. DISCUSSION

The NMR and EPR results of Section III can be combined to provide the following picture of vanadium metals deposition on a Co–Mo/γ-Al_2O_3 catalyst during the HDS process. At low loadings the VO^{2+} species dominates, a form different from that encountered in crude oils or on calcined supports and involving sulfur as one component of its environment. The maximum level of VO^{2+} observed appears to be in the vicinity of 0.7 wt%. This maximum loading and the invariance of the width of the signal suggests that these paramagnetic VO^{2+} species are isolated, perhaps residing at defect sites on the Al_2O_3 support. At higher loadings a diamagnetic vanadium species is observed by NMR. The irregularity of the absorption signal suggests a number of physically (and possibly chemically) inequivalent sites for the vanadium atom. Intensity studies indicate a maximum loading of this species on the catalyst of ~6 to 10 wt%, suggesting that it may exist as a monolayer on the surface of the catalyst. The composition of this phase cannot be determined from the present observations, but conditions of deposition would be favorable for a sulfide or oxysulfide phase. For loadings beyond ~10 wt%, the balance of the vanadium occurs as a vanadium sulfide with a composition very close to V_2S_3. The large metals capacity of heavily loaded catalysts before deactivation suggest that these sulfides are depositing as crystallites rather than as a surface phase. X-Ray observations of these spent catalysts indicate

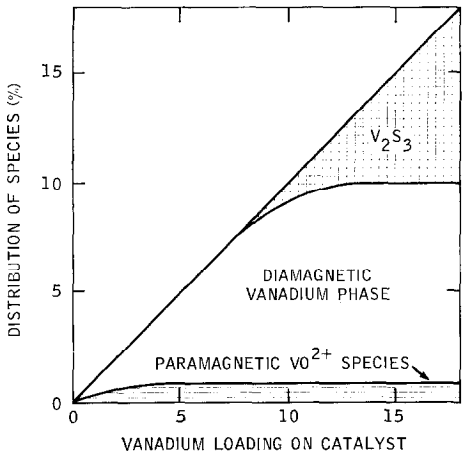

FIG. 6. Schematic picture of the successive stages of vanadium deposition during the HDS process.

lines which can be indexed on the vanadium sulfide phase (*20*) and scanning electron microscopy shows platelets typical of V_2S_3 (*21*). Crystal formation could lead to pore blockage and limit catalyst lifetime. This deposition pattern is summarized schematically in Fig. 6. This pattern is independent of feed and catalyst support types for typical HDS conditions described in Section II. Temperature and hydrogen pressure have not been systematically varied and changes could possibly modify this deposition sequence.

In summary, magnetic resonance techniques, NMR and EPR, have been used in combination to probe the microscopic chemistry of vanadium deposition during the HDS process. Comparison with observations on model system has permitted the identification of the chemical forms of vanadium occurring on the catalyst. Different vanadium phases occur and their deposition appears to be progressive. The occurrence of a crystalline V_2S_3 phase at high metals loading suggests that catalyst deactivation by pore plugging is the ultimate cause of deactivation of these catalysts.

ACKNOWLEDGMENTS

The following colleagues have been generous in their discussion of various aspects of this work and for providing selected samples: R. R. Chianelli, J. P. de Neufville, F. R. Gamble, J. D. Paynter, T. A. Pecoraro, W. K. Robbins, and A. H. Thompson. L. A. Gebhard assisted in the accumulation and interpretation of the resonance data, and J. R. Alonzo has surveyed the samples with scanning electron microscopy.

REFERENCES

1. Kwan, T., and Sato, M., *Nippon Kagaka Zasshi* **19**, 1103 (1970).
2. Nikishenko, S. B., Brodskii, E. S., Vail, Yu. K., Bobkovskii, E. I., and Manshilin, V. V., *Int. Chem. Eng.* **16**, 320 (1976).
3. See, e.g., de Vries, A. B., and Jellinek, F., *Rev. Chim. Min.* **11**, 624 (1974).
4. de Vries, A. B., and Haas, C., *J. Phys. Chem. Solids* **34**, 651 (1973).
5. Silbernagel, B. G., Levy, R. B., and Gamble, F. R., *Phys. Rev.* **B11**, 4563 (1975).
6. Silbernagel, B. G., and Thompson, A. H., *Physica* **B86–88**, 1003 (1977).
7. Silbernagel, B. G., and Thompson, A. H., *Bull. Amer. Phys. Soc.* **22**, 422 (1977).
8. de Neufville, J. P., Ruppert, A. F., and Silbernagel, B. G., *Bull. Amer. Phys. Soc.* **22**, 422 (1977).
9. We are most grateful to J. D. Paynter of the Exxon Research and Development Laboratories for the use of these samples.
10. Drain, L. E., *Metal Rev.* **119**, 195 (1967).
11. Kivelson, D., and Lee, S. K., *J. Chem. Phys.* **41**, 1896 (1964).
12. See, e.g., Selbin, J., *Coord. Chem. Revs.* **1**, 293 (1966).
13. McConnell, H. M., Porterfield, W. W., and Robertson, R. E., *J. Chem. Phys.* **30**, 442 (1959).
14. Boucher, L. J., Tynan, E. C., and Yen, T. F., in "Electron Spin Resonance of Metal Complexes," p. 111, Plenum, New York, 1969.
15. Yen, T. F., Boucher, L. J., Dickie, J. P., Tynan, E. C., and Vaughan, G. B., *J. Inst. Petrol.* **55**, 87 (1969).
16. Yen, T. F., Tynan, E. C., Vaughan, G. B., and Boucher, L. J., in "Spectrometry of Fuels," p. 187. Plenum, New York, 1970.
17. See, e.g., Vorotyntsev, V. M., Shuets, V. A., and Kazanaskii, V. B., *Kinet. Katal.* **12**, 678 (1971).
18. van Reijen, L. L., and Cossee, P., *Disc. Faraday Soc.* **41**, 277 (1966).
19. Silbernagel, B. G., to be published.
20. R. R. Chianelli, private communication.
21. J. R. Alonzo, private communication.